Systematic Biases in Tropical Drought Monitoring: Rethinking SPI Application in Mesoamerica's Humid Regions

Article *in* Meteorology · July 2025

DOI: 10.3390/meteorology4030018

2 authors:

David Romero
National Autonomous University of Mexico
31 PUBLICATIONS **218** CITATIONS
SEE PROFILE

Eric Alfaro
University of Costa Rica
287 PUBLICATIONS **5,658** CITATIONS
SEE PROFILE

meteorology

Article

Systematic Biases in Tropical Drought Monitoring: Rethinking SPI Application in Mesoamerica's Humid Regions

David Romero and Eric J. Alfaro

MDPI

https://doi.org/10.3390/meteorology4030018

meteorology

MDPI

Article

Systematic Biases in Tropical Drought Monitoring: Rethinking SPI Application in Mesoamerica's Humid Regions

David Romero [1,*] and Eric J. Alfaro [2,3]

[1] Escuela Nacional de Estudios Superiores, Unidad Mérida, Universidad Nacional Autónoma de México, Carretera Merida-Tetiz, km 4, Ucu 97357, Yucatan, Mexico
[2] Centro de Investigaciones Geofísicas (CIGEFI), Universidad de Costa Rica, San José 11505, Costa Rica; erick.alfaro@ucr.ac.cr
[3] Centro de Investigación en Ciencias del Mar y Limnología (CIMAR), Universidad de Costa Rica, San José 11501, Costa Rica
* Correspondence: dromero@enesmerida.unam.mx

Abstract

The Standardized Precipitation Index (SPI) is widely used to determine drought severity worldwide. However, inconsistencies exist regarding its application in warm, humid tropical climatic zones. Originally developed for temperate regions with a continental climate, the index may not adequately reflect drought conditions in tropical environments where rainfall regimes differ substantially. This study identifies the following two principal reasons why the traditional calculation method fails to characterize drought severity in tropical domains: first, the marked humidity contrast between the consistently humid rainy season and the rest of the year, and second, the diverse drought types in tropical regions, which include both long-term and short-term events. Using data from meteorological stations in Mexico's humid tropics and comparing them with temperate regions, the study demonstrates significant discrepancies between SPI-based drought classifications and actual precipitation patterns. Our analysis shows that the abundant precipitation during the rainy season causes biases in longer time scales integrated into multivariate drought indices. Considerations are established for adapting the SPI for decision makers who monitor drought in humid tropics, with specific recommendations on time scale limits to avoid biases. This work contributes to more accurate drought monitoring in tropical regions by addressing the unique climatic characteristics of these environments.

Keywords: drought; tropical climate; precipitation regime; SPI; México

Academic Editors: Paul D. Williams and Adrianos Retalis

Received: 30 April 2025
Revised: 21 June 2025
Accepted: 3 July 2025
Published: 8 July 2025

Citation: Romero, D.; Alfaro, E.J. Systematic Biases in Tropical Drought Monitoring: Rethinking SPI Application in Mesoamerica's Humid Regions. *Meteorology* **2025**, *4*, 18. https://doi.org/10.3390/meteorology4030018

1. Introduction

Natural disasters cause increasingly costly damage to human infrastructure worldwide [1]. Among these disasters, drought affects the largest territorial extension [2] and impacts multiple sectors, including agriculture, economy, human health, and water resources. In tropical regions, drought monitoring faces unique challenges due to pronounced seasonal precipitation contrasts, yet existing drought indices were developed for temperate climates with fundamentally different rainfall regimes [3,4]. This mismatch between index design and the characteristics of tropical climates raises critical questions about the accuracy of drought assessments in these regions.

To quantify drought severity, researchers have developed various indices to measure drought as a function of time [5,6]. The Palmer Drought Severity Index (PDSI) [7] and the Standardized Precipitation Index (SPI) [8] remain among the most widely used

indices [9,10]. However, the PDSI is rarely implemented in low- and middle-income tropical countries because it requires extensive data beyond precipitation, including evapotranspiration, runoff, and soil moisture information [11], which is often unavailable or incomplete in these regions. Additionally, the PDSI has shown inconsistencies in drought trend measurements in tropical areas [12] and is not well suited for regions experiencing wide variations in precipitation or temperature extremes [5].

The SPI offers an alternative that only requires precipitation data, making it more accessible for tropical countries where such data can be obtained from international or national databases. Consequently, it has been recommended for drought studies in tropical domains like Mexico [13,14] and is used as a reference for drought response policies in Mexico for comprehensive and preventive management [15].

However, since the SPI is based solely on precipitation, it may overestimate or underestimate drought characteristics under changing climatic conditions. Recent studies have highlighted additional concerns about the SPI's performance under global warming scenarios. Vicente-Serrano et al. [9] demonstrated that rising temperatures increase atmospheric evaporative demand, making precipitation-only indices insufficient for capturing actual drought severity. Trenberth et al. [16] demonstrated that global warming intensifies the hydrological cycle, resulting in more extreme precipitation events that can mask underlying drought trends when using precipitation-based indices. Similarly, Cook et al. [17] found that temperature-driven increases in evapotranspiration demand can create "hot droughts" that the SPI fails to detect adequately. These limitations are particularly pronounced in tropical regions, where high temperatures and humidity create complex interactions between precipitation patterns and actual water availability [18,19].

Indeed, a significant knowledge gap exists regarding the suitability of the SPI for tropical regions. The index was originally developed in the temperate United States (specifically Iowa, Kansas, and North Dakota), where climatic conditions differ markedly from those of tropical regions. While the SPI can be calculated for periods ranging from 1 to 48 months, previous research has raised questions about its universal applicability. Sanz Donaire [20] identified potential high positive biases when calculating the index for all months without the consideration of seasonal patterns. This raises important questions about the SPI's effectiveness in tropical regions, where precipitation regimes differ significantly from those in temperate zones.

Differences in atmospheric circulation between tropical and temperate regions create distinct precipitation regimes that affect how drought develops and manifests [21]. These differences are critical to understanding why drought indices developed for temperate regions may perform poorly in tropical environments [22]. In tropical areas, atmospheric circulation dominated by the Hadley cell creates seasonal precipitation patterns that are fundamentally different from those in temperate zones [23]. The seasonal migration of the Intertropical Convergence Zone (ITCZ) creates pronounced wet and dry seasons in many tropical regions, including Mexico and Central America [24]. Unlike mid-latitude regions where frontal systems dominate precipitation mechanisms [Hoskins], tropical areas experience convective precipitation driven by solar heating and moisture convergence [25]. Additional tropical weather systems, such as easterly waves, synoptic gyres, and tropical cyclones, significantly contribute to the total annual rainfall in Mesoamerica [26–28]. In western Mexico, the North American Monsoon significantly modifies summer precipitation patterns, bringing pronounced wet seasons that contrast sharply with temperate precipitation regimes [29].

In contrast, temperate regions experience atmospheric circulation dominated by the prevailing westerlies and transient mid-latitude cyclones [30]. Precipitation mechanisms vary distinctly by season and place. In the central U.S., during spring, the Great Plains

Low-Level Jet drives moisture convergence, creating conditions favorable for frontal and convective precipitation systems along boundaries where warm, moist air masses collide with cooler, drier air [31]. Summer precipitation shifts to a regime dominated by diurnal heating and localized convection, resulting in isolated thunderstorms that are less organized than those in spring [31]. Cold-season precipitation is limited by the moisture-holding capacity of colder air, creating natural constraints on precipitation intensity. Overall, precipitation tends to be more evenly distributed throughout the year in temperate regions outside monsoon-influenced areas.

These fundamental differences in precipitation mechanisms affect how drought develops. In temperate regions, drought often evolves gradually as persistent high-pressure systems block frontal passages over extended periods, with deficits accumulating progressively throughout the year [32]. In monsoon-influenced regions, delayed onset or weakened monsoon circulation can quickly lead to significant drought conditions during what should be the wettest period of the year [33]. In tropical regions, the timing of precipitation deficits is critical—deficits during the dry season may limit hydrological significance, while deficits during the expected wet season can rapidly lead to agricultural and hydrological impacts [34]. Changes in rain event frequency often matter more than total precipitation volume; reducing the number of rainy days during the wet season can create "hidden droughts" that impact agriculture even if seasonal totals remain near normal [34]. The convective nature of tropical rainfall and sharp seasonal transitions can lead to more rapid drought onset and recovery than in temperate regions [35]. Additionally, in tropical forests, a significant portion of precipitation originates from local evapotranspiration, which can be disrupted during dry periods, thereby intensifying drought conditions through feedback mechanisms that are less prominent in temperate areas.

These meteorological differences pose a challenge to the application of standardized drought indices which were developed for temperate climates. While the SPI mathematically standardizes precipitation anomalies relative to local climate, it does not account for these fundamental differences in precipitation mechanisms, timing significance, and drought development processes. Despite being standardized to climatological normal [36] to theoretically remove seasonal trends, the SPI may not adequately capture the unique characteristics of tropical precipitation patterns or monsoon-influenced regions. In areas affected by the North American Monsoon, standard drought indices may not properly represent the rapid transitions between dry and wet conditions or the critical importance of monsoon timing and intensity. Similarly, in tropical regions, the pronounced seasonal contrast between wet and dry periods, as well as the different types of droughts (mid-summer and pre-summer droughts), creates conditions that may compromise the SPI's effectiveness at certain time scales.

The SPI-12 (calculated over 12 months) is commonly used in Mexico to determine meteorological drought risk and vulnerability across large hydrological basins [37]. However, this approach may not adequately reflect the complex drought dynamics in tropical regions, where drought can manifest at different temporal scales and with varying impacts.

Therefore, this study aims to establish a framework for appropriate use of the SPI in warm, humid tropics, enabling decision makers to monitor droughts more accurately in tropical regions by considering their unique climatic characteristics. The specific objectives are as follows:

- Examine the climatic differences between temperate and tropical regions that affect drought index performance.
- Analyze the performance of SPI-based drought classifications in Mexico's humid tropics by comparing them with observed water balance conditions.

- Identify systematic biases in SPI application at different time scales in tropical environments.
- Define time scale limits that should be considered to avoid biases in tropical drought monitoring.
- Provide recommendations for adapting the SPI to better reflect tropical drought conditions.

The rest of the paper is organized as follows. Section 2 describes the study area, focusing on Mexico's warm, humid tropical regions, presents the data sources, including the Mexico Drought Monitor and meteorological databases, and outlines the methodology for comparing SPI-based drought classifications with observed water balance conditions. Section 3 presents the results, first comparing drought monitor classifications with in situ water balance data to identify inconsistencies, then analyzing the critical climatic differences between tropical and temperate regions during their respective rainy seasons. Section 4 discusses the implications of the findings for drought monitoring in tropical regions, examining the methodological limitations of applying the SPI at longer time scales in these environments. Finally, Section 5 concludes with specific recommendations for adapting SPI application in tropical climates, including suggested time scale limits to avoid biases in drought monitoring systems.

2. Materials and Methods

2.1. Study Area and Climatic Context

This study is focused on the lowlands of the warm, humid tropical area of Mexico. Warm, tropical megathermal climates, ranging from humid to sub-humid, correspond to Group A of the Köppen–Geiger classification [38]. Tropical megathermal climates (Group A) have a mean monthly temperature of 18 °C or higher, with an annual precipitation exceeding potential evapotranspiration, distinguishing them from Group B climates (dry, warm deserts or semi-arid steppes). The rainfall regime defines the specific climate types within Group A. The Af classification represents a tropical forest climate characterized by an average monthly rainfall of at least 60 mm. The Am category indicates a tropical monsoon climate with a driest month precipitation less than 60 mm but higher than (100 mm − (total annual precipitation/25)). Finally, the Aw classification denotes a humid and dry tropical climate characterized by the driest month having rainfall below the preceding rule.

Mexican tropical lowlands contain all three Group A climate types [39]. Aw is present in the Yucatan Peninsula and both coastal areas, extending inland to the state of Morelos; Af occurs in the foothills of the southern mountains; and Am forms a buffer zone between these two (Figure 1).

These tropical regions experience two distinct types of drought within the annual precipitation cycle. The first is mid-summer drought ("veranillo" or "canícula" in Spanish), which is a relatively short period (less than 2 months, typically July–August) of decreased rainfall during the rainy season, accompanied by high temperatures. This phenomenon is influenced by different factors depending on the region. Along the Pacific coast, it relates to variations in the location and intensity of the ITCZ in the eastern Pacific [40]. In the Gulf of Mexico and Caribbean areas, it is affected by expansion and shifts in the North Atlantic Subtropical High (NASH), which cuts off moisture transport into the Caribbean [41]. Vulnerability to mid-summer drought depends on its duration and the soil's water retention capacity [12,42].

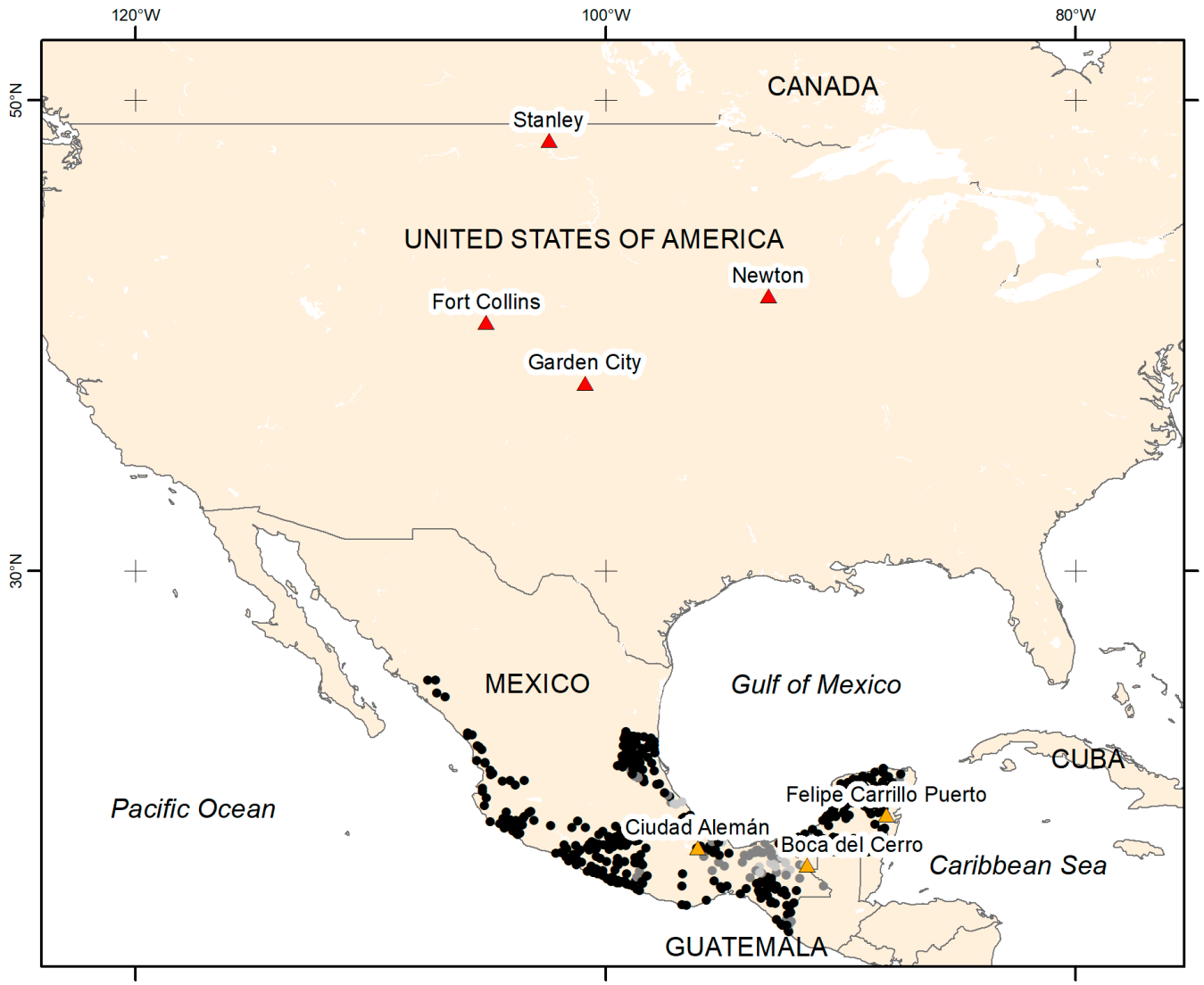

Figure 1. Maps with localization of the CliCOM study stations (black dot, Aw climate stations, middle gray Am, light gray Af), Mexican retained stations (orange triangle), and U.S. stations (red triangle) (Table 1).

Table 1. Typical meteorological stations representative of tropical and temperate regions (Figure 1).

Station	State	Climate	Data Period	Years of Available Data
Felipe Carrillo Puerto	Quintana Roo—MX	Aw	1952–2019	65
Ciudad Alemán	Veracruz—MX	Am	1951–2020	70
Boca del Cerro	Tabasco—MX	Af	1948–2019	68
Garden City	Kansas—USA	Cfa	1950–2015	71
Newton	Iowa—USA	Dfa	1893–2016	76
Stanley	North Dakota—USA	Dfb	1938–2016	74
Fort Collins	Colorado—USA		1998–2024	26

The second type is pre-summer drought, which exhibits a slow, prolonged development that begins in the cooler winter–spring period at the end of the rainy season and is characterized by occasional precipitation from cold fronts. This can be divided into the following two subcategories: "winter" drought, which depends on cold front activity from the end of the rainy season (October–November) to its usual onset the next year (May–

June), and delayed summer rainfall onset, which occurs when the rainy season begins later than usual.

Although temporally continuous, these drought types have different impacts on human activities. Winter drought affects honey production, permanent crops, and livestock and increases forest fire risk, while summer rainfall delays primarily impact rainfed crops.

These drought types represent different temporal scales and characteristics that challenge the uniform application of drought indices developed for temperate regions. Their distinct patterns and impacts necessitate specialized approaches to drought monitoring and management in tropical Mexican environments.

2.2. Data Sources

2.2.1. Mexico Drought Monitor

A drought index is a quantitative measure that characterizes the severity, duration, and spatial extent of drought conditions by integrating meteorological, hydrological, or agricultural variables into a single numerical value. Drought indices serve as standardized tools for monitoring water deficits, comparing drought conditions across different regions and time periods, and supporting decision making in water resource management and agricultural planning.

The Mexico Drought Monitor utilizes a composite drought index that combines multiple indicators to assess drought severity. This multivariate approach combines the Standardized Precipitation Index (SPI) calculated at various time scales (1, 3, 6, and 12 months) with additional hydrological and soil moisture indicators [43]. The resulting composite index is then translated into the following five discrete drought intensity categories: D0 (abnormally dry), D1 (moderate drought), D2 (severe drought), D3 (extreme drought), and D4 (exceptional drought). These classifications follow the same framework used by the North American Drought Monitor. They are designed to reflect the impacts of water deficits on different sectors, including agriculture, water supply, and natural ecosystems.

Drought index values are assigned at the municipal level and represent the predominant drought conditions within each administrative unit. These classifications are reported on the last day of each month, starting from January 2003, with mid-month values available from 15 February 2014. This approach enables regional drought monitoring and policy implementation, but it may mask local-scale variability in actual water availability conditions, particularly in regions with diverse topography or microclimates. This database is accessible at smn.cna.gob.mx/es/climatologia/monitor-de-sequia/monitor-de-sequia-en-mexico (accessed on 10 April 2025).

2.2.2. Meteorological Data

We utilized the national climatological database for Mexico, which was integrated into the Climate Computing project (CliCOM) and is maintained by the National Meteorological Service of Mexico (SMN). Daily observations at 5459 stations are recorded at 08:00 local time, representing the previous 24 h. The CliCOM data series extends from 1902 to 2022, with varying coverage periods for each station (median of 32 years). The data include daily and monthly minimum and maximum temperature (°C) values, precipitation and evaporation (mm), as well as various meteorological phenomena. Few stations have complete time series for the ultimate normal period of 1991–2020 [36,44], consequently, we selected stations with at least 30 years of data since 1981. In total, 485 stations matched the requirement and represent Group A climate regions (Figure 1). Additionally, we identified the longest time series for each climate type for more detailed analysis (Table 1, Figure 1).

To compare tropical and temperate conditions, historical rainfall and temperature data were obtained from GHCN-D databases [45–47] for Fort Collins, the place for which the

SPI was originally developed [8], and stations from regions where the SPI authors tested the index [48], including central Iowa, west Kansas, and northeast North Dakota, with different climates (Table 1, Figure 1).

The daily precipitation and temperature data were processed using R version 4.5 [49] to compute monthly values. To ensure data quality, a minimum of 80% of daily observations was required to create a valid monthly value, and any missing data were flagged during analysis.

2.3. Methods

2.3.1. Conceptual Framework

Understanding drought conditions in tropical regions requires careful consideration of the complete water balance, which encompasses not only precipitation inputs, but also evapotranspiration losses. This study employed several key water balance components that are fundamental to assessing actual water availability conditions [50,51]. Indeed, this study employed water balance calculations rather than precipitation alone to avoid circular reasoning, since the SPI derives exclusively from precipitation data. Water balance provides an independent, physically based assessment of actual water availability that accounts for both water inputs (precipitation) and atmospheric demand (evapotranspiration).

This methodological choice addresses the issue in defining drought in terms of statistical precipitation anomalies or actual water stress conditions. In tropical regions, periods classified as statistically "dry" can still maintain an unneglectable water balance due to high absolute precipitation levels. Conversely, statistically "normal" precipitation during times of high demand may lead to water deficits.

This approach compares the following two drought assessment paradigms: (1) the statistical method (SPI) based on precipitation anomalies relative to historical norms and the derived Mexico Drought Monitor, and (2) the physical method (water balance) based on actual water supply versus demand. Instances where these methods did not provide similar results—particularly drought classifications during substantial water surpluses—may indicate biases in SPI application.

Potential evapotranspiration (PET) represents the maximum amount of water that could be evaporated and transpired from a vegetated surface if water supply was unlimited [52]. PET is primarily controlled by atmospheric demand factors, including temperature, humidity, wind speed, and solar radiation [53]. In tropical regions, PET remains relatively high and consistent throughout the year due to persistent warm temperatures and abundant solar energy, typically ranging from 100 to 150 mm per month [54].

Actual evapotranspiration (AET) represents the actual amount of water that is evaporated and transpired under existing environmental conditions, including water availability constraints [55]. AET is always less than or equal to PET, with the difference depending on soil moisture availability, vegetation characteristics, and atmospheric conditions [56]. During periods of water stress, AET becomes significantly lower than PET as plants close stomata and reduce transpiration to conserve water [57].

Water balance (S) is the difference between precipitation and AET losses [58]. Positive water balance values indicate water surplus conditions where precipitation exceeds evapotranspiration demands, leading to soil moisture recharge, runoff, and groundwater recharge.

These water balance components provide a physically based assessment of water availability that complements statistical drought indices like the SPI [59]. While the SPI identifies precipitation anomalies relative to historical norms, the water balance approach evaluates whether the actual water supply meets atmospheric demand, providing a more direct measure of hydrological stress [60]. This distinction is particularly important in tropical re-

gions, where even statistically "dry" periods may still maintain positive water balances due to high absolute precipitation amounts, while statistically "normal" precipitation during high-demand periods may result in water deficits [61].

2.3.2. Water Balance (S) Calculations

PET complete time series are generally lacking in the CliCOM database; consequently, to obtain monthly potential evapotranspiration, this study applied the Hargreaves–Samani formula [62] (1) to compute the daily PET for the 15th day of each month, PET_d, using mean monthly temperature and extraterrestrial radiation values for this representative mid-month date. The monthly PET calculation multiplies this daily value by the number of days in each month.

$$PET_d = 0.0023 \times Ra \times (Tm + 17.8) \times (Tx - Tn)^{0.5} \quad (1)$$

where Tm is the mean temperature (°C), Tx is the maximum temperature (°C), Tn is the minimum temperature (°C), and Ra is the extraterrestrial radiation (mm per day), which was calculated based on the Julian day, latitude, and solar parameters.

Since potential evapotranspiration represents the maximum limits that may not occur in reality, we calculated actual evapotranspiration (AET) using Budyko's dimensionless relationship [58] (2).

$$AET = [P/PET \times \tanh(PET/P) \times (1 - \exp(-PET/P))]^{0.5} \quad (2)$$

where P is the monthly accumulated precipitation and PET is the potential evapotranspiration.

The monthly water balance was then calculated as (3).

$$S = P - AET \quad (3)$$

where S is the water balance (mm), P is the total monthly precipitation (mm), and AET is the actual monthly evapotranspiration (mm).

2.4. Standardized Precipitation Index (SPI)

The SPI is based on the long-term precipitation record for a specific location and time scale. The index represents the number of standard deviations that observed precipitation deviates from the long-term mean for a normally distributed random variable [63].

The SPI calculation involves fitting precipitation data to a probability distribution and transforming the results to standard normal values. Precipitation data are first aggregated over the desired time scale (1, 3, 6, 12, or more months). The aggregated precipitation data are then fitted to a probability distribution, with the gamma distribution being most commonly used due to its flexibility in modeling precipitation data and its ability to handle the skewed, positive nature of precipitation records [64]).

The gamma probability density function using rate parameterization is expressed in Equation (4), as follows:

$$f(x) = (\lambda^{\alpha}/\Gamma(\alpha)) \times x^{\alpha-1} \times e^{-\lambda x} \quad (4)$$

where $\alpha > 0$ is the shape parameter, $\lambda > 0$ is the rate parameter, $x > 0$ is the precipitation amount, and $\Gamma(\alpha)$ is the gamma function. In this parameterization, the mean equals α/λ and the variance equals α/λ^2.

Parameter estimation for the gamma distribution requires robust methods due to the complex nature of precipitation data, which often includes zero values, extreme events, and seasonal variations. Maximum likelihood estimation (MLE) provides optimal parameter estimates by maximizing the likelihood function, making it superior to simpler methods like

the method of moments, particularly when dealing with skewed precipitation distributions and limited sample sizes [64]. The MLE approach is especially important for SPI calculations because parameter accuracy directly affects the reliability of drought classifications.

For the rate parameterization, MLE estimates are obtained by solving the system of Equations (5) and (6), as follows:

$$\partial \ln L/\partial \alpha = n[\psi(\alpha) - \ln(\lambda)] + \Sigma \ln(xi) = 0 \quad (5)$$

$$\partial \ln L/\partial \lambda = n\alpha/\lambda - \Sigma xi = 0 \quad (6)$$

where $\psi(\alpha)$ is the digamma function and L is the likelihood function. From Equation (7), the rate parameter can be expressed as follows:

$$\lambda = n\alpha/\Sigma xi = \alpha/\bar{x} \quad (7)$$

where $\bar{x}$ is the sample mean. The shape parameter α is then solved iteratively using numerical methods, as no closed-form solution exists for Equation (5).

The cumulative probability G(x) is calculated using the fitted gamma distribution parameters. Finally, this cumulative probability is transformed to a standard normal distribution using the inverse normal function (8):

$$SPI = 1/\Phi(G(x)) \quad (8)$$

where $1/\Phi$ is the inverse standard normal cumulative distribution function.

For each of the 485 Mexican stations, we calculated SPI values at multiple time scales (1, 3, 6, 9, 12, and 24 months) using maximum likelihood estimation implemented in the fitdistrplus package in R [65]. This approach ensured robust parameter estimation across the diverse precipitation regimes represented in our dataset.

The SPI classifies drought intensity as follows:

- SPI ≥ -0.5: Near normal to wet conditions
- $-1.0 \leq$ SPI < -0.5: Mild drought
- $-1.5 \leq$ SPI < -1.0: Moderate drought
- $-2.0 \leq$ SPI < -1.5: Severe drought
- SPI < -2.0: Extreme drought

The SPI assumes that precipitation follows a gamma distribution, that the time series is stationary, and that the standardization removes seasonal effects. However, in tropical regions with pronounced seasonal rainfall patterns, these assumptions may be violated, particularly when calculating the SPI over time scales that span multiple seasons with dramatically different precipitation regimes. The use of MLE becomes even more critical in these environments, as it provides the most robust parameter estimates when distributional assumptions are challenged by extreme seasonal variability (4). Indeed, McKee et al. [8] and Beguería y Vicente-Serrano [66] used the method of moments, but this is not adequate when $\alpha > 10$ [64].

2.5. Comparative Analysis Framework

2.5.1. Mexico Drought Monitor vs. Water Surplus

To evaluate the application of the SPI in tropical regions, we compared municipal-scale SPI-based drought classifications from the Mexico Drought Monitor with observed precipitation data from meteorological stations. We matched each of the 330 Group A climate stations with their corresponding municipality's drought classification and analyzed instances where drought was reported during periods of significant precipitation.

For this purpose, water surplus conditions were defined using a water balance threshold of 100 mm, calculated as the difference between monthly precipitation and evapotranspiration. A water balance threshold of 100 mm was established as a critical value to identify significant water surplus conditions in tropical regions following a multi-criteria approach. This threshold represents a biophysically significant quantity that indicates a sufficient water availability to prevent drought conditions in tropical ecosystems, regardless of statistical precipitation anomalies [50,67]. For the more severe thresholds (200 mm, 300 mm, etc.) used later, these values were established as incremental benchmarks to demonstrate the magnitude of misclassification, showing that drought was reported even during periods of extraordinary water surplus that would make any meaningful definition of drought implausible in these tropical ecosystems [68,69]. Indeed, instances where drought was reported during months with a water balance exceeding 100 mm were identified as potential inconsistencies.

2.5.2. Climatic Conditions Comparison

To understand the underlying causes of these inconsistencies, we compared the climatic characteristics of tropical (Mexico) and temperate (USA) regions by analyzing precipitation variability during the typical wettest three-month period in each region and examining seasonal water balance patterns. We analyzed each station's available data record for the three wettest consecutive months to capture long-term variability. This approach enabled the identification of critical differences in precipitation regimes that might affect SPI performance. Also, by comparing these climatic parameters, we aimed to isolate the specific factors contributing to potential biases in SPI calculations in tropical regions and develop recommendations for appropriate time scales for drought monitoring. The comparison between temperate and tropical precipitation regimes during their respective wettest periods serves to quantify the fundamental climatic differences that render the SPI inappropriate for tropical applications. This analysis may demonstrate that even the minimum recorded precipitation values during tropical wet seasons substantially exceed the median values observed in temperate regions where the SPI was developed, creating statistical distributions that violate the assumptions underlying SPI calculations and explaining why tropical 'drought' classifications often coincide with actual water surplus conditions.

2.5.3. Heteroscedasticity Assessment

To quantify the seasonal variance differences that affect SPI validity, we calculated the Heteroscedasticity Index (HI) for each station following established methods for detecting non-constant variance in time series data [70,71], an approach that has been applied to hydrological time series to assess stationarity assumptions [72]. Wet and dry season precipitation statistics were computed separately for each station and then combined to assess the variance stability assumptions underlying SPI calculations. Wet and dry seasons were defined based on regional climate patterns. For Mexican tropical stations, the wet season encompasses months 6–10 (June through October), corresponding to the primary rainy season influenced by the North American Monsoon and ITCZ positioning. The dry season spans from November to May and is characterized by high-pressure systems and reduced convective activity. For U.S. temperate stations, the wet season is defined as months 4–9 (April through September), reflecting the period of maximum precipitation from spring frontal systems and summer convective activity. The dry season corresponds to months 10–3 (October through March), when cold-season precipitation is limited by reduced atmospheric moisture capacity.

For each station, wet season variance (σ^2_wet) and dry season variance (σ^2_dry) were calculated using (9) and (10), as follows:

$$\sigma^2\_wet = Var(P\_wet) \quad (9)$$

$$\sigma^2\_dry = Var(P\_dry) \quad (10)$$

where P_wet and P_dry represent precipitation during wet and dry seasons, respectively.

The Heteroscedasticity Index was then computed as follows (11):

$$HI = \sigma^2\_wet / \sigma^2\_dry \quad (11)$$

Values of HI $\approx$ 1 indicate homoscedastic conditions suitable for SPI application, while HI >> 1 or HI << 1 indicate heteroscedastic conditions that violate SPI stationarity assumptions. This metric provides a quantitative measure of seasonal precipitation variance stability, which directly relates to the validity of SPI calculations.

2.5.4. Gamma Distribution Parameter Analysis

To examine the statistical distributions underlying SPI calculations, gamma distribution parameters were estimated for each station using maximum likelihood estimation (MLE) [73]. This methodology adheres to established procedures for drought index development [8] and offers robust parameter estimation for the entire precipitation time series [74]. The analysis utilized the fitdistrplus package in R to estimate the shape parameter (α) and rate parameter (λ) for the gamma distribution fitted to each station's complete precipitation dataset.

These parameters characterize the distributional properties that SPI calculations assume remain consistent across the time series. A comparative analysis was conducted between tropical and temperate stations using Mann–Whitney U tests to assess significant differences in distributional parameters between the two climate types.

2.5.5. False Drought Classification Analysis

We developed a framework to quantify SPI performance by identifying instances where drought classifications occurred during actual water surplus conditions.

False drought events were defined as follows (12):

$$P(\text{False Drought}) = P(SPI < -1.0 \cap S > 100 \text{ mm}) \quad (12)$$

where SPI < -1.0 represents moderate to severe drought classification and S > 100 mm indicates substantial water surplus conditions. This probability was calculated for each time scale and station combination to assess systematic bias patterns.

The false drought probability metric provides direct validation of SPI accuracy by comparing statistical drought classifications with physically based water availability assessments. This approach avoids circular reasoning by using independent measures (water balance) to validate precipitation-based indices.

3. Results

3.1. Mexico Drought Monitor vs. In Situ Water Balance Data

The comparison of drought classifications with calculated water balance values revealed numerous inconsistencies. We identified 2939 instances where a municipality was classified as experiencing drought (at any level) during a month when the corresponding weather stations' average recorded a water balance of at least 100 mm (Table 2). These occurrences were distributed across 272 municipalities and spanned 140 months (58.3%

of the monitoring period). Inconsistencies were particularly pronounced during months with a high water surplus, with drought reported even when the monthly water balance exceeded 500 mm, for instance, in 2010, two municipalities of Chiapas reported extreme drought for May and June (Unión Juárez) and June and July (Tapachula). However, during these periods, the water balances were 1476.2 and 1378.4 mm, respectively.

Table 2. Events with monthly water balance > 100 mm at a meteorological station in Mexico, in terms of the Mexico Drought Monitor municipal drought index.

Water Balance Threshold (mm)	Drought Index				
	Abnormally Dry	Moderate Drought	Severe Drought	Extreme Drought	Exceptional Drought
100	1054	537	218	56	5
200	327	184	79	29	0
300	130	59	34	6	0
400	63	22	15	4	0
500	58	36	15	8	0

Figure 2a presents two complementary maps that illustrate the geographical distribution of drought classification inconsistencies across Mexico. The upper map displays the frequency of misclassification events in each municipality, highlighting areas where drought was reported despite water balance measurements exceeding 100 mm. This frequency map reveals that municipalities with the highest number of misclassification incidents are concentrated in the southern tropical regions, particularly along the coastlines. The states of Chiapas, Tabasco, and Veracruz exhibit the most pronounced discrepancies, with numerous municipalities experiencing more than 20 months of misclassification during the study period.

These regions are primarily characterized by the wettest climate types (Am and Af), where intense seasonal rainfall generates substantial water surpluses.

The map in Figure 2b illustrates the severity of drought classifications assigned during periods of water surplus. It shows that even the most severe drought categories (exceptional and extreme drought) were incorrectly applied to regions experiencing substantial water surpluses, particularly in southern Mexico. The concentration of red and orange coloration in states such as Chiapas indicates that these areas not only experienced frequent misclassifications, but also the most severe category errors in drought reporting. This pattern suggests that the standardized indices struggle most significantly in regions with the most pronounced tropical rainfall characteristics.

The case of the Chiapas municipalities (Unión Juárez and Tapachula) being classified as experiencing extreme drought in 2010 despite recording extraordinary water balances exceeding 1300 mm provides an example of this phenomenon. These municipalities, located in Mexico's southernmost state with a tropical climate influenced by mountain orography, exemplify how the conventional drought monitoring framework fails to capture the actual water availability conditions in such regions. Similar patterns are present along both the Gulf of Mexico and Pacific coastal zones, where the interaction between tropical moisture sources and local topography creates precipitation regimes fundamentally different from those for which drought indices were originally designed.

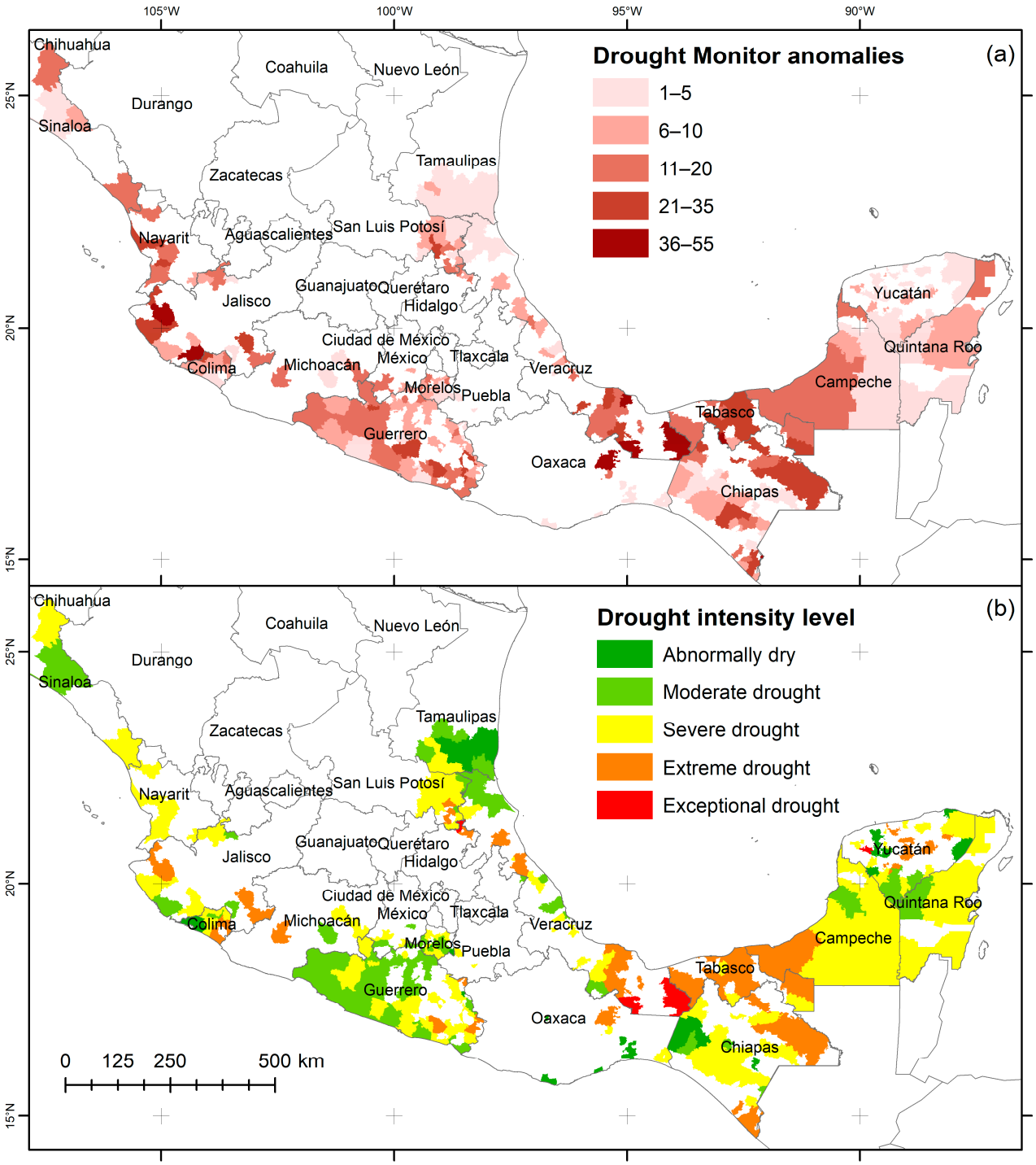

Figure 2. (**a**) Number of months with drought monitor anomalies per municipality and (**b**) highest drought intensity level reported during a month with water balance > 100 mm.

3.2. Critical Climatic Differences Between Temperate and Tropical Regions Rainy Seasons

The boxplot (Figure 3) illustrates the differences in precipitation volumes during the wettest three-month periods for the seven stations. Notably, even the minimum recorded precipitation values at tropical Mexican stations (such as the 244 mm recorded at Felipe Carrillo Puerto in 1957) substantially exceed the median values observed at Fort Collins and Stanley. This minimum value in tropical regions, despite representing a significant negative anomaly that would generate an SPI-3 value of −2.15 (categorized as "exceptional drought"), still provides more absolute water input than what would be considered normal conditions in temperate zones. The interquartile ranges show minimal overlap between the

two climate types, with tropical stations consistently receiving 2–3 times more precipitation during their wet seasons than temperate stations. Furthermore, the tropical stations exhibit extraordinary maximum values, with some locations recording over 1000 mm during particularly intense rainy seasons.

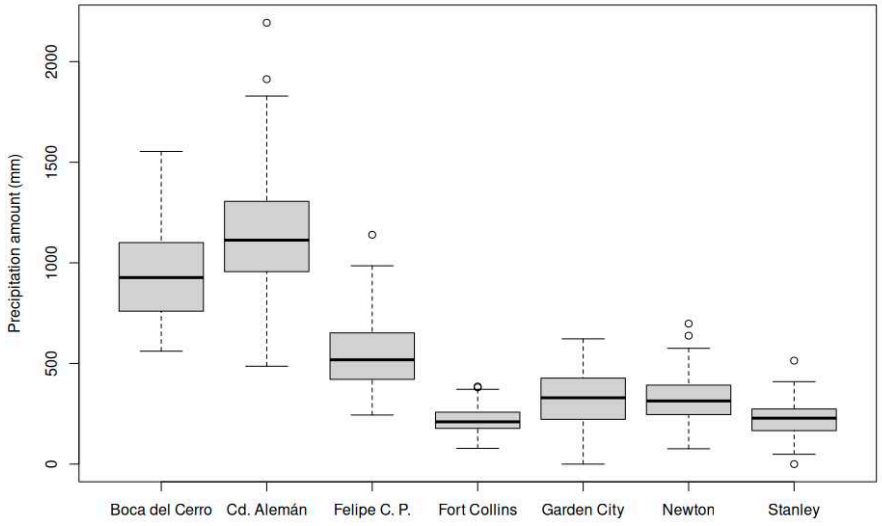

Figure 3. Boxplot of annual rainfall for the three wettest consecutive months from 1952. Mexican stations: August–October; U.S. stations: May–July. Dots are outliers.

Figure 4 reveals that tropical Mexican stations maintain substantially higher water balances during their wettest periods compared to temperate U.S. stations, with minimal overlap between their respective distributions. Even during statistically "dry" years, tropical stations typically maintain positive water balances that significantly exceed the median values observed at temperate stations. Only Felipe Carrillo Puerto has values under 200 mm, with a minimum of 58.4 mm in 1970. In contrast, Garden City Newton and Stanley have various years with a water balance under 5 mm.

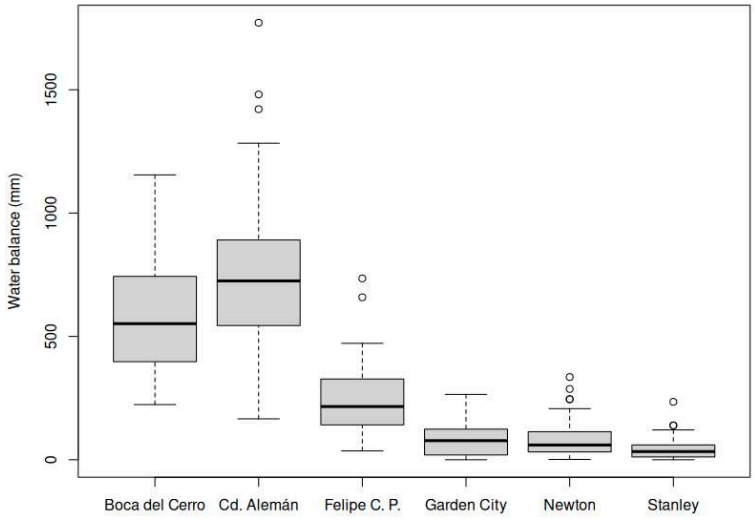

Figure 4. Boxplot of annual water balance for the three wettest consecutive months from 1952. Mexican stations: August–October; U.S. stations: May–July. Dot are outliers.

Additionally, the interquartile range for tropical stations consistently shows water surpluses above 400 mm, whereas temperate stations rarely exceed this threshold, even during their wettest periods.

The analysis of the wettest three-month periods (August–October for Mexican stations and May–July for US stations) revealed fundamental differences between tropical and temperate precipitation regimes that challenge SPI assumptions. The minimum recorded precipitation during tropical wet seasons (244 mm at Felipe Carrillo Puerto in 1957) exceeded the median precipitation of temperate wet seasons (60.9 mm) by a factor of 4:1. More strikingly, this tropical minimum value exceeded even the maximum temperate wet-season precipitation (76.8 mm) by a ratio of 3.18:1, demonstrating that even the most extreme "drought" conditions during tropical wet seasons provide more absolute water input than normal temperate conditions.

These discrepancies likely stem from fundamental methodological limitations in applying the SPI to tropical climates.

The SPI and derived drought monitoring systems were primarily developed for and in temperate regions, where precipitation is more evenly distributed throughout the year. In tropical regions, pronounced seasonality creates a distinct hydrological reality where statistical anomalies may not necessarily translate to actual drought conditions.

3.3. Mathematical Analysis of SPI Performance

The heteroscedasticity analysis confirms that tropical precipitation has fundamentally different statistical properties compared to temperate precipitation. The Heteroscedasticity Index revealed pronounced differences between climate types, with tropical stations exhibiting mean HI values of 5.43 compared to 0.658 for temperate stations. Individual tropical stations demonstrated HI values ranging from 2.16 (Boca del Cerro) to 11.85 (Ciudad Alemán), indicating that the variance in wet-season precipitation was 2–12 times greater than that in the dry season. In contrast, temperate stations exhibited relatively stable variance ratios (0.542–0.869), with variances during the wet and dry seasons remaining comparable.

The coefficient of variation analysis reinforced these findings, with tropical stations showing CV ratios ranging from 0.485 to 0.589. In contrast, temperate stations exhibited greater variability in CV ratios (-0.356 to 0.240), including negative values indicating a lower relative variability during the wet season. This heteroscedasticity violates the stationarity assumptions underlying gamma distribution fitting in SPI calculations, which explains why standardized indices fail to accurately represent actual drought conditions in tropical regions.

The maximum likelihood estimation of gamma distribution parameters revealed systematic differences between tropical and temperate precipitation that affect the validity of SPI calculations. Tropical stations demonstrated shape parameters ranging from 0.710 to 1.540 (mean = 1.142), while temperate stations showed higher shape parameters ranging from 1.646 to 2.376 (mean = 1.993). The rate parameters showed even more pronounced differences, with tropical stations exhibiting rates ranging from 0.0042 to 0.0105 (mean = 0.0076) compared to temperate stations, which had rates ranging from 0.1113 to 0.1955 (mean = 0.1470). These distributional differences suggest that a single gamma distribution may not adequately represent the full range of precipitation conditions in tropical climates.

3.4. Station-Specific Drought Index Performance

The false drought classification analysis revealed systematic increases in misclassification probability with longer SPI time scales, particularly at tropical stations. While the 1-month SPI showed zero false drought probability for all tropical stations, longer time scales demonstrated an increasing bias with substantial inter-station variation.

At the 3-month scale, tropical stations maintained zero false drought probability, while temperate stations showed minimal rates (0.13–0.31%, mean = 0.21%). However, pronounced differences emerged at longer scales. For the 6-month SPI, tropical stations showed false drought probabilities ranging from 0.00% (Felipe Carrillo Puerto) to 1.31% (Boca del Cerro), with a mean of 0.52%. At 9-month scales, tropical stations demonstrated dramatic increases, with probabilities ranging from 0.26% to 6.42% (mean = 3.70%), whereas temperate stations remained relatively stable, with probabilities ranging from 0.30% to 1.38% (mean = 0.92%).

The most pronounced station-specific differences were observed at the 12-month and 24-month scales. Felipe Carrillo Puerto, the driest station with an Aw climate, consistently demonstrated the lowest false drought rates across all scales, reaching only 0.40% at 12 months and 0.81% at 24 months. Conversely, Ciudad Alemán showed the highest 12-month false drought rate (2.96%), while Boca del Cerro exhibited the highest 24-month rate (4.02%). These patterns indicate that Felipe Carrillo Puerto, the driest tropical station, can accommodate longer SPI calculations with minimal bias. In contrast, wetter tropical stations, such as Boca del Cerro and Ciudad Alemán, require shorter time scale limits.

The analysis reveals that appropriate SPI time scale limits vary substantially by station characteristics rather than following universal recommendations. Tropical stations, as a group, showed false drought probabilities exceeding 2% at both 12-month (mean = 2.00%) and 24-month (mean = 2.95%) scales, whereas temperate stations maintained consistently low rates ($\leq$0.36%) across all time scales. These findings suggest that SPI application in tropical regions requires station-specific validation and potentially shorter time scale limits for drought monitoring.

4. Discussion

4.1. Implications for Tropical Drought Monitoring

Effective drought monitoring requires consideration of both the type of drought and the usual climatic conditions of a location. Under normal conditions, drought represents a low-frequency event [12,75], defined as a significant deficit in expected precipitation patterns that impacts water availability for human activities and ecosystems. This consideration is particularly important for agriculture in tropical regions, where planting dates are scheduled to coincide with the expected onset of seasonal rains.

A standardized index like the SPI is theoretically ideal for monitoring such deficits, since it normalizes precipitation relative to local climate norms. However, our results indicate that in regions with Type A climates, particularly those with pronounced seasonal rainfall patterns, the calculation of multivariate SPI for periods up to 24 months (as used in parts of our study area by Gómez Díaz et al. [76] and for Mexico generally by Servicio Meteorológico Nacional [43]) may not accurately indicate drought conditions.

SPI application at longer time scales in tropical regions suffers from two fundamental issues that align with previous critiques of precipitation-only indices. The abundant rainy-season precipitation creates statistical biases that mask developing drought conditions [77,78], while extreme seasonal contrasts violate the stationarity assumptions underlying SPI calculations [72]. These findings support Svoboda et al. [79], who argued that single-variable indices are insufficient to capture the complexity of drought in diverse climatic regions. This statistical issue corroborates recent advances in the development of drought indices. Stagge et al. [80] and Blain et al. [81] demonstrated the importance of climate-specific probability distributions, while Beguería et al. [82] showed that incorporating temperature variables significantly improves drought detection in water-limited environments. Our tropical findings extend these concerns to humid regions, where precipitation abundance, rather than scarcity, creates index performance issues.

Our overall findings align with research by Livada & Assimakopoulos [83] in temperate regions and Le et al. [84] in tropical domains, who found a varying effectiveness of drought indices at different time scales across regions with distinct rainfall regimes. Similarly, Quesada-Hernández et al. [75] noted that different drought indices produced significantly different estimates of drought extent in the Central American Dry Corridor, highlighting the need for regionally appropriate indices.

In a recent study assessing corn grain production under drought conditions in eastern Mexico using the Mexican Drought Monitor [85], it is notable that the good correlations obtained by the authors correspond to the arid zones of the study region. In contrast, in areas with Type A climates, the relationships between the drought monitor level and production were considerably lower. This provides additional evidence that current drought monitoring approaches may not accurately reflect the impacts on agriculture in tropical climates.

The first heavy rains in tropical areas with pronounced rainy seasons effectively end any pre-summer drought, regardless of cumulative precipitation deficits. During the rainy season, the length of dry spells and rainfall efficiency are better indicators of drought conditions than monthly anomalies. For regions experiencing mid-summer drought, a monthly index may fail to capture these shorter-term events, which typically last less than one month. This rapid drought termination contradicts the gradual recovery patterns assumed by longer SPI time scales. This supports Hayes et al. [86] and Wilhite [87], who emphasized that drought characteristics vary fundamentally across climate zones. Agricultural studies in similar climates [88,89] confirm that rainfall timing and intensity matter more than cumulative anomalies for crop impacts.

The soil water capacity exceedance during tropical wet seasons creates conditions incompatible with drought definitions, regardless of statistical precipitation rankings. This aligns with Sheffield et al. [90], who advocated for physically based drought assessment approaches, and Vicente-Serrano et al. [9], who demonstrated that evapotranspiration-based indices better capture actual water stress conditions.

These mathematical findings support a nuanced approach to SPI modification in tropical regions rather than universal time scale restrictions. The analysis suggests implementing station-specific temporal thresholds based on local false drought probability patterns: conservative 4–6-month limits for stations exhibiting high heteroscedasticity (HI > 10), moderate 8–10-month limits for intermediate stations (HI = 2–10), and potentially longer limits for stations with lower seasonal variance contrasts (HI < 2). This approach acknowledges the climatic diversity within tropical regions while addressing the systematic biases identified in standard SPI applications.

The quantitative validation demonstrates that SPI bias in tropical regions results from fundamental statistical incompatibilities rather than calibration issues, requiring methodological adaptation rather than parameter adjustment to achieve accurate drought monitoring in these critical climate zones.

These findings demonstrate that tropical drought monitoring requires fundamental modifications to current standardized approaches. A 6- to 8-month SPI threshold is recommended here for pre-summer drought monitoring, reflecting the need to exclude rainy-season influence while maintaining a sufficient temporal scope for meaningful trend detection [91]. For mid-summer drought events, SPI-1 or sub-monthly indices better capture the rapid onset characteristic of these phenomena [92]. This climate-specific approach aligns with recent calls for regionally adapted drought indices [5,93] and addresses the disconnect between the statistical anomalies and actual agricultural impacts observed in tropical Mexico [85]. The implementation of such tailored approaches could prevent

the misallocation of drought response resources during periods of actual water surplus, improving both scientific accuracy and policy effectiveness.

4.2. Study Limitations

This study acknowledges limitations that should be considered when interpreting the results and applying the recommendations. First, the analysis relies on point meteorological measurements that may not fully represent the spatial variability within municipalities, particularly in topographically complex regions where elevation gradients create microclimatic differences [94]. The municipal-scale drought classifications used may, therefore, introduce spatial-scale mismatches when compared to station-specific water balance calculations.

Second, the water balance approach, although physically based, employs simplified evapotranspiration calculations using the Hargreaves–Samani method, which may underestimate the actual evapotranspiration in humid tropical environments compared to more complex methods, such as the Penman–Monteith method [51]. The use of mid-month radiation and monthly temperature values to represent entire months introduces temporal averaging effects that may not capture daily-scale variations in atmospheric demand, which are critical for short-term drought assessment.

Third, the 100 mm water balance threshold, although conservative and justified for tropical conditions, represents an arbitrary cutoff that may not be universally applicable across all tropical subregions or soil types. Different ecosystems and agricultural systems may experience water stress at varying threshold levels depending on rooting depth, soil water holding capacity, and crop water requirements [95].

Finally, this analysis focuses exclusively on meteorological drought and does not address the impacts of hydrological, agricultural, or socioeconomic droughts, which may respond differently to precipitation anomalies. The relationship between meteorological conditions and actual drought impacts varies considerably across sectors and may not follow the patterns identified here [87].

4.3. Future Research Directions

This study opens several avenues for advancing drought monitoring in tropical regions. However, it is important to recognize that the SPI will likely continue to be used in operational contexts because the concept of drought in meteorological monitoring is not necessarily related to a lack of water to maintain a healthy environment, but rather serves as an index that indicates an anomaly in the rainfall regime with respect to its median [96]. This distinction between meteorological anomalies and actual water stress conditions represents a fundamental conceptual challenge that future research must address.

Given this reality, research should focus on developing complementary approaches rather than the wholesale replacement of existing systems. First, expanded geographical validation is needed to test the proposed SPI modifications across diverse tropical climates beyond Mexico, including the Amazon basin, Southeast Asia, and tropical Africa, where different monsoon systems and precipitation regimes may require additional adaptations [19]. It involves working at the local level and adjusting the SPI thresholds to more accurately identify drought conditions—those characterized by actual precipitation deficits and associated impacts—in order to better support decision makers.

Second, the development of hybrid drought indices specifically designed for tropical regions represents a critical research priority. Such indices should integrate precipitation patterns, evapotranspiration dynamics, and soil moisture characteristics while maintaining compatibility with existing SPI-based monitoring systems [97,98]. Machine learning approaches could optimize the weighting of these variables based on regional climate characteristics and drought impact relationships.

Third, real-time implementation studies are essential to validate the practical applicability of the proposed 8-month SPI threshold and sub-monthly indices for mid-summer drought detection. Pilot programs, in collaboration with national meteorological services, could assess the operational feasibility and user acceptance of modified drought monitoring protocols while maintaining consistency with international reporting standards [99].

Fourth, research should focus on developing decision support frameworks that help users to interpret SPI values within the context of actual water availability conditions. This includes creating region-specific guidance on when SPI anomalies translate to meaningful hydrological or agricultural impacts [100].

Finally, interdisciplinary research is needed to link meteorological drought indices with assessments of agricultural, hydrological, and socioeconomic impacts in order to validate whether the proposed modifications better predict actual drought consequences in tropical regions [101]. This includes developing region-specific vulnerability assessments that take into account local adaptive capacity and drought management practices.

5. Conclusions

This study provides the first systematic validation of SPI performance against physical water balance conditions in tropical regions, demonstrating systematic biases that reveal fundamental incompatibilities between temperate-designed indices and tropical climate characteristics. While previous studies have questioned the applicability of the SPI in various climates [75,83,84], this work uniquely quantifies the magnitude and mechanisms of systematic bias through a comparison of statistical drought classifications with independently calculated water availability.

Three key findings establish the novelty and significance of this research. First, unlike previous descriptive studies of drought index performance [13,14,76], this work documents 2939 instances of drought reported during substantial water surplus conditions (>100 mm monthly balance) across 272 Mexican municipalities—the largest-scale validation of SPI accuracy in tropical regions to date. These misclassifications occurred even during extreme water surpluses exceeding 1300 mm, indicating a profound disconnection between statistical precipitation anomalies and physical drought conditions.

Second, while other studies have noted SPI limitations in monsoon-influenced regions [33,84], this research uniquely identifies specific temporal thresholds necessary to prevent systematic bias. The 8-month SPI threshold recommended here for pre-summer drought monitoring represents the first empirically derived, operationally applicable guideline based on actual meteorological data spanning various decades, moving beyond the largely theoretical recommendations of previous studies [20,80,81].

Third, this work establishes a direct comparison between temperate and tropical precipitation regimes specifically designed to explain drought index performance differences. The analysis demonstrates that the minimum precipitation during tropical wet periods exceeds median temperate values, making standardized drought thresholds meaningless when applied across climate zones—a mechanism that explains why tropical "drought" classifications often coincide with conditions representing water abundance in temperate regions.

Author Contributions: Conceptualization, D.R. and E.J.A.; methodology, D.R.; software, D.R.; formal analysis, D.R. and E.J.A.; investigation, D.R.; resources, D.R.; data curation, D.R.; writing—original draft preparation, D.R.; writing—review and editing, D.R. and E.J.A.; visualization, D.R.; supervision, D.R.; project administration, D.R.; funding acquisition, D.R. and E.J.A. All authors have read and agreed to the published version of the manuscript.

Funding: Research was funded by UNAM-PAPIIT IA302220, Universidad de Costa Rica grants: A4906 (PESCTMA), C4226 (Eco-Salud), C3991 (UCREA), B0-810, C2103 and funding by a grant awarded by the International Development Research Centre (IDRC), Ottawa, Canada, and the Central American University Council (CSUCA-SICA) to the Red Centroamericana de Ciencias sobre Cambio Climático (RC4) project (CR-66, C4468, SIA0054-2). The APC was funded by MDPI.

Institutional Review Board Statement: Not applicable.

Informed Consent Statement: Not applicable.

Data Availability Statement: Data are available at Global Historical Climate Network Daily web page https://www.ncei.noaa.gov/products/land-based-station/global-historical-climatology-network-daily (accessed on 10 April 2025), at CliCOM web page cucapa-clicom.cicese.mx/ (accessed on 10 April 2025) and Monitor de Sequía de México /smn.conagua.gob.mx/es/climatologia/monitor-de-sequia/monitor-de-sequia-en-mexico (accessed on 10 April 2025).

Acknowledgments: D.R. thanks the program UNAM-PAPIIT IA302220. E.J.A. wish to acknowledge the funding of this research through the following Vicerrectoría de Investigación, Universidad de Costa Rica grants: A4906 (PESCTMA), C4226 (Eco-Salud), C3991 (UCREA), B0-810, C2103 and funding by a grant awarded by the International Development Research Centre (IDRC), Ottawa, Canada, and the Central American University Council (CSUCA-SICA) to the Red Centroamericana de Ciencias sobre Cambio Climático (RC4) project (CR-66, C4468, SIA0054-2, the opinions expressed here do not necessarily represent those of IDRC, CSUCA, or the Board of Governors). To the UCR research center CIGEFI for their logistic support during the data compilation and analysis.

Conflicts of Interest: The authors declare no conflicts of interest. The funders had no role in the design of the study; in the collection, analyses, or interpretation of data; in the writing of the manuscript; or in the decision to publish the results.

Abbreviations

The following abbreviations are used in this manuscript:

PDSI	Palmer Drought Severity Index
SPI	Standardized Precipitation Index
ITCZ	Intertropical Convergence Zone
NASH	North Atlantic Subtropical High
PET	Potential Evapotranspiration
AET	Actual Evapotranspiration
HI	Heteroscedasticity Index
MLE	Maximum Likelihood Estimation

References

1. CRED EM-DAT. The International Disasters Database of the Centre for Research on the Epidemiology of Disasters. Available online: https://public.emdat.be/ (accessed on 25 January 2024).
2. Wilhite, D.A. Drought as a Natural Hazard: Concepts and Definitions. In *Drought: A Global Assessment*; Routledge: London, UK, 2000; pp. 3–18.
3. Esparza, M. Drought and Water Shortages in Mexico. Current Status and Future Prospects. *Secuencia* **2014**, *89*, 193–219.
4. Graniel, C.E.; Irany, V.M.; Gonzalez Hita, L. Dinámica de La Interfase Salina y Calidad Del Agua En La Costa Nororiental de Yucatán. *Artic. Investig.* **2004**, *3*, 15–25.
5. Hayes, M.J. Drought Indices. In *Van Nostrand's Scientific Encyclopedia*; John Wiley & Sons, Inc.: Hoboken, NJ, USA, 2005; ISBN 978-0-471-74398-9.
6. Keyantash, J.; Dracup, J.A. The Quantification of Drought: An Evaluation of Drought Indices. *Bull. Am. Meteorol. Soc.* **2002**, *83*, 1167–1180. [CrossRef]
7. Palmer, W.C. *Meteorological Drought*; Research Paper No. 45; US Department of Commerce; Weather Bureau: Washington, DC, USA, 1965; Volume 30.

8. McKee, T.B.; Doesken, N.J.; Kleist, J. The Relationship of Drought Frequency and Duration to Time Scales. In Proceedings of the 8th Conference on Applied Climatology, Anaheim, CA, USA, 17–22 January 1993; American Meteorological Society: Boston, MA, USA, 1993; Volume 17, pp. 179–183.
9. Vicente-Serrano, S.M.; Beguería, S.; López-Moreno, J.I. A Multiscalar Drought Index Sensitive to Global Warming: The Standardized Precipitation Evapotranspiration Index. *J. Clim.* **2010**, *23*, 1696–1718. [CrossRef]
10. Tatli, H. Multivariate-Drought Indices—Case Studies with Observations and Outputs of NCAR CCSM-4 Ensemble Models. *Theor. Appl. Climatol.* **2021**, *146*, 257–275. [CrossRef]
11. Guttman, N.B. Comparing the Palmer Drought Index and the Standardized Precipitation Index. *J. Am. Water Resour. Assoc.* **1998**, *34*, 113–121. [CrossRef]
12. Hidalgo, H.G.; Alfaro, E.J.; Amador, J.A.; Bastidas, Á. Precursors of Quasi-Decadal Dry-Spells in the Central America Dry Corridor. *Clim. Dyn.* **2019**, *53*, 1307–1322. [CrossRef]
13. Giddings, L.; Soto, M.; Rutherford, B.M.; Maarouf, A. Standardized Precipitation Index Zones for México. *Atmosfera* **2005**, *18*, 33–56.
14. Fernandes, F.A.C.; Santos, L.O.F.D.; Nunes, N.D.C.; Machado, N.G.; Biudes, M.S. Quantifying Droughts in Mato Grosso with SPI and SPEI: Exploring Connections to Tropical Sea Surface Temperatures. *Theor. Appl. Climatol.* **2024**, *155*, 9751–9766. [CrossRef]
15. Aguilar-Barajas, I.; Sisto, N.P.; Magaña-Rueda, V.; Ramírez, A.I.; Mahlknecht, J. Drought Policy in Mexico: A Long, Slow March toward an Integrated and Preventive Management Model. *Water Policy* **2016**, *18*, 107–121. [CrossRef]
16. Trenberth, K.E.; Dai, A.; Van Der Schrier, G.; Jones, P.D.; Barichivich, J.; Briffa, K.R.; Sheffield, J. Global Warming and Changes in Drought. *Nat. Clim. Change* **2014**, *4*, 17–22. [CrossRef]
17. Cook, B.I.; Smerdon, J.E.; Seager, R.; Coats, S. Global Warming and 21st Century Drying. *Clim. Dyn.* **2014**, *43*, 2607–2627. [CrossRef]
18. Williams, A.P.; Cook, E.R.; Smerdon, J.E.; Cook, B.I.; Abatzoglou, J.T.; Bolles, K.; Baek, S.H.; Badger, A.M.; Livneh, B. Large Contribution from Anthropogenic Warming to an Emerging North American Megadrought. *Science* **2020**, *368*, 314–318. [CrossRef] [PubMed]
19. Mukherjee, S.; Mishra, A.; Trenberth, K.E. Climate Change and Drought: A Perspective on Drought Indices. *Curr. Clim. Change Rep.* **2018**, *4*, 145–163. [CrossRef]
20. Sanz Donaire, J.J. El Índice Xerocórico. Un Indicador Geográfico de La Sequía Pluviométrica (España y Polonia). *Estud. Geogr.* **2007**, *68*, 679–708. [CrossRef]
21. Holton, J.R.; Hakim, G.J. *An Introduction to Dynamic Meteorology*; Academic Press: Cambridge, MA, USA, 2013; Volume 88.
22. Dai, A. Characteristics and Trends in Various Forms of the Palmer Drought Severity Index During 1900–2008. *J. Geophys. Res.* **2011**, *116*, D12115. [CrossRef]
23. Walker, C.C.; Schneider, T. Eddy Influences on Hadley Circulations: Simulations with an Idealized GCM. *J. Atmospheric Sci.* **2006**, *63*, 3333–3350. [CrossRef]
24. Waliser, D.E.; Gautier, C. A Satellite-Derived Climatology of the ITCZ. *J. Clim.* **1993**, *6*, 2162–2174. [CrossRef]
25. Romatschke, U.; Houze, R.A. Extreme Summer Convection in South America. *J. Clim.* **2010**, *23*, 3761–3791. [CrossRef]
26. Khouakhi, A.; Villarini, G.; Vecchi, G.A. Contribution of Tropical Cyclones to Rainfall at the Global Scale. *J. Clim.* **2017**, *30*, 359–372. [CrossRef]
27. Spracklen, D.V.; Arnold, S.R.; Taylor, C.M. Observations of Increased Tropical Rainfall Preceded by Air Passage over Forests. *Nature* **2012**, *489*, 282–285. [CrossRef] [PubMed]
28. Papin, P.P.; Bosart, L.F.; Torn, R.D. A Climatology of Central American Gyres. *Mon. Weather Rev.* **2017**, *145*, 1983–2000. [CrossRef]
29. Adams, D.K.; Comrie, A.C. The North American Monsoon. *Bull. Am. Meteorol. Soc.* **1997**, *78*, 2197–2213. [CrossRef]
30. Feldmann, M.; Emanuel, K.; Zhu, L.; Lohmann, U. Estimation of Atlantic Tropical Cyclone Rainfall Frequency in the United States. *J. Appl. Meteorol. Climatol.* **2019**, *58*, 1853–1866. [CrossRef]
31. Chen, L.; Ford, T.W.; Swenson, E. The Role of the Circulation Patterns in Projected Changes in Spring and Summer Precipitation Extremes in the U.S. Midwest. *J. Clim.* **2023**, *36*, 1943–1956. [CrossRef]
32. Seager, R.; Hoerling, M. Atmosphere and Ocean Origins of North American Droughts. *J. Clim.* **2014**, *27*, 4581–4606. [CrossRef]
33. Ashfaq, M.; Shi, Y.; Tung, W.; Trapp, R.J.; Gao, X.; Pal, J.S.; Diffenbaugh, N.S. Suppression of South Asian Summer Monsoon Precipitation in the 21st Century. *Geophys. Res. Lett.* **2009**, *36*, 2008GL036500. [CrossRef]
34. Zeng, D.; Yuan, X. The Important Role of Reduced Moisture Supplies from the Monsoon Region in the Formation of Spring and Summer Droughts over Northeast China. *J. Clim.* **2024**, *37*, 1703–1722. [CrossRef]
35. Fang, Y.; Leung, L.R.; Wolfe, B.T.; Detto, M.; Knox, R.G.; McDowell, N.G.; Grossiord, C.; Xu, C.; Christoffersen, B.O.; Gentine, P.; et al. Disentangling the Effects of Vapor Pressure Deficit and Soil Water Availability on Canopy Conductance in a Seasonal Tropical Forest During the 2015 El Niño Drought. *J. Geophys. Res. Atmos.* **2021**, *126*, e2021JD035004. [CrossRef]
36. World Meteorological Organization. *Guide to Climatological Practices*; WMO: Geneva, Switzerland, 2023; Volume 100.

37. Neri, C.; Magaña, V. Estimation of Vulnerability and Risk to Meteorological Drought in Mexico. *Weather Clim. Soc.* **2016**, *8*, 95–110. [CrossRef]
38. Geiger, R. Klassifikation Der Klimate Nach, W. Köppen [Classification of Climates According to W. Köppen]. In *Astronomie und Geophysik*; Landolt-Börnstein-Zahlenwerte Funkt. Aus Phys. Chem. Astron. Geophys. Tech. Alte Ser. [Landolt-Börnstein-Fig. Funct. Phys. Chem. Astron. Geophys. Technol. Old Ser]; Springer: Berlin/Heidelberg, Germany, 1954; Volume 3, Part III; pp. 603–607.
39. Vidal, R. *Las Regiones Climáticas de México*; Temas selectos de la Geografía de México; Instituto de Geografía UNAM: México, DF, Mexico, 2005.
40. García-Franco, J.L.; Chadwick, R.; Gray, L.J.; Osprey, S.; Adams, D.K. Revisiting Mechanisms of the Mesoamerican Midsummer Drought. *Clim. Dyn.* **2023**, *60*, 549–569. [CrossRef]
41. Martinez, C.; Kushnir, Y.; Goddard, L.; Ting, M. Interannual Variability of the Early and Late-Rainy Seasons in the Caribbean. *Clim. Dyn.* **2020**, *55*, 1563–1583. [CrossRef]
42. Romero, D.; Torres-Irineo, E.; Kern, S.; Orellana, R.; Hernandez-Cerda, M.E. Determination of the Soil Moisture Recession Constant from Satellite Data: A Case Study of the Yucatan Peninsula. *Int. J. Remote Sens.* **2017**, *38*, 5793–5813. [CrossRef]
43. Servicio Meteorológico Nacional Monitor de Sequía en México. Available online: https://smn.cna.gob.mx/es/climatologia/monitor-de-sequia/monitor-de-sequia-en-mexico (accessed on 10 April 2025).
44. Arguez, A.; Vose, R.S. The Definition of the Standard WMO Climate Normal. *Bull. Am. Meteorol. Soc.* **2011**, *92*, 699–704. [CrossRef]
45. Durre, I.; Menne, M.J.; Gleason, B.E.; Houston, T.G.; Vose, R.S. Comprehensive Automated Quality Assurance of Daily Surface Observations. *J. Appl. Meteorol. Climatol.* **2010**, *49*, 1615–1633. [CrossRef]
46. Durre, I.; Squires, M.F.; Vose, R.S.; Yin, X.; Arguez, A.; Applequist, S. NOAA's 1981-2010 U.S. Climate Normals: Monthly Precipitation, Snowfall, and Snow Depth. *J. Appl. Meteorol. Climatol.* **2013**, *52*, 2377–2395. [CrossRef]
47. Menne, M.J.; Durre, I.; Korzeniewski, B.; McNeal, S.; Thomas, K.; Yin, X.; Anthony, S.; Ray, R.; Vose, R.S.; Gleason, B.E.; et al. Global Historical Climatology Network-Daily (GHCN-Daily), Version 3. *NOAA Natl. Clim. Data Cent.* **2012**, *10*, V5D21VHZ.
48. Edwards, D.C.; McKee, T.B. *Characteristics of 20th Century Drought in the United States at Multiple Time Scales*; Colorado State University: Fort Collins, CO, USA, 1997.
49. R Core Team. *R: A Language and Environment for Statistical Computing*; R Foundation for Statistical Computing: Vienna, Austria, 2025.
50. Ma, Y.-J.; Shi, F.-Z.; Hu, X.; Li, X.-Y. Threshold Vegetation Greenness under Water Balance in Different Desert Areas over the Silk Road Economic Belt. *Remote Sens.* **2020**, *12*, 2452. [CrossRef]
51. Allen, R.G.; Pereira, L.S.; Raes, D.; Smith, M. *Crop Evapotranspiration—Guidelines for Computing Crop Water Requirements—FAO Irrigation and Drainage Paper 56*; FAO: Rome, Italy, 1998; Volume 300, p. D05109.
52. Penman, H.L. Natural Evaporation from Open Water, Bare Soil and Grass. *Proc. R. Soc. Lond. Ser. Math. Phys. Sci.* **1948**, *193*, 120–145.
53. Monteith, J.L. Evaporation and Environment. In *Proceedings of the Symposia of the Society for Experimental Biology*; Cambridge University Press (CUP): Cambridge, UK, 1965; Volume 19, pp. 205–234.
54. Fisher, J.B.; Melton, F.; Middleton, E.; Hain, C.; Anderson, M.; Allen, R.; McCabe, M.F.; Hook, S.; Baldocchi, D.; Townsend, P.A.; et al. The Future of Evapotranspiration: Global Requirements for Ecosystem Functioning, Carbon and Climate Feedbacks, Agricultural Management, and Water Resources. *Water Resour. Res.* **2017**, *53*, 2618–2626. [CrossRef]
55. Zhang, K.; Kimball, J.S.; Running, S.W. A Review of Remote Sensing Based Actual Evapotranspiration Estimation. *WIREs Water* **2016**, *3*, 834–853. [CrossRef]
56. Priestley, C.H.B.; Taylor, R.J. On the Assessment of Surface Heat Flux and Evaporation Using Large-Scale Parameters. *Mon. Weather Rev.* **1972**, *100*, 81–92. [CrossRef]
57. Jones, H.G. *Plants and Microclimate: A Quantitative Approach to Environmental Plant Physiology*; Cambridge University Press: Cambridge, UK, 2014.
58. He, G.; Zhao, Y.; Wang, J.; Gao, X.; He, F.; Li, H.; Zhai, J.; Wang, Q.; Zhu, Y. Attribution Analysis Based on Budyko Hypothesis for Land Evapotranspiration Change in the Loess Plateau, China. *J. Arid Land* **2019**, *11*, 939–953. [CrossRef]
59. Cramer, W.; Kicklighter, D.W.; Bondeau, A.; Iii, B.M.; Churkina, G.; Nemry, B.; Ruimy, A.; Schloss, A.L.; ThE. Participants OF. ThE. Potsdam NpP. Model Intercomparison. Comparing Global Models of Terrestrial Net Primary Productivity (NPP): Overview and Key Results. *Glob. Change Biol.* **1999**, *5*, 1–15. [CrossRef]
60. Vicente-Serrano, S.M.; Beguería, S.; López-Moreno, J.I.; Angulo, M.; El Kenawy, A. A New Global 0.5° Gridded Dataset (1901–2006) of a Multiscalar Drought Index: Comparison with Current Drought Index Datasets Based on the Palmer Drought Severity Index. *J. Hydrometeorol.* **2010**, *11*, 1033–1043. [CrossRef]
61. Porporato, A.; Daly, E.; Rodriguez-Iturbe, I. Soil Water Balance and Ecosystem Response to Climate Change. *Am. Nat.* **2004**, *164*, 625–632. [CrossRef]
62. Hargreaves, G.H.; Samani, Z.A. Reference Crop Evapotranspiration from Temperature. *Appl. Eng. Agric.* **1985**, *1*, 96–99. [CrossRef]

63. Svoboda, M.; Hayes, M.; Wood, D. *Standardized Precipitation Index: User Guide*; World Meteorological Organization: Geneva, Switzerland, 2012.
64. Wilks, D.S. *Statistical Methods in the Atmospheric Sciences*, 4th ed.; Elsevier: Amsterdam, The Netherlands; Cambridge, MA, USA, 2019; ISBN 978-0-12-815823-4.
65. Delignette-Muller, M.L.; Dutang, C. Fitdistrplus: An R Package for Fitting Distributions. *J. Stat. Softw.* **2015**, *64*, 1–34. [CrossRef]
66. Beguería, S.; Vicente-Serrano, S.M. SPEI: Calculation of the Standardized Precipitation-Evapotranspiration Index. 2025. Available online: https://cran.r-project.org/web//packages//SPEI/SPEI.pdf (accessed on 9 April 2025).
67. Scarpati, O.E.; Spescha, L.B.; Lay, J.A.F.; Capriolo, A.D. Soil Water Surplus in Salado River Basin and Its Variability during the Last Forty Years (Buenos Aires Province, Argentina). *Water* **2011**, *3*, 132–145. [CrossRef]
68. Casagrande, E.; Recanati, F.; Rulli, M.C.; Bevacqua, D.; Melià, P. Water Balance Partitioning for Ecosystem Service Assessment. A Case Study in the Amazon. *Ecol. Indic.* **2021**, *121*, 107155. [CrossRef]
69. Yao, S.; Zhao, C.; Zhou, J.; Li, Q. The Association of Drought with Different Precipitation Grades in the Inner Mongolia Region of Northern China. *Water* **2024**, *16*, 3292. [CrossRef]
70. Breusch, T.S.; Pagan, A.R. A Simple Test for Heteroscedasticity and Random Coefficient Variation. *Econom. J. Econom. Soc.* **1979**, *47*, 1287–1294. [CrossRef]
71. White, H. A Heteroskedasticity-Consistent Covariance Matrix Estimator and a Direct Test for Heteroskedasticity. *Econom. J. Econom. Soc.* **1980**, *48*, 817–838. [CrossRef]
72. Serinaldi, F.; Kilsby, C.G.; Lombardo, F. Untenable Nonstationarity: An Assessment of the Fitness for Purpose of Trend Tests in Hydrology. *Adv. Water Resour.* **2018**, *111*, 132–155. [CrossRef]
73. Husak, G.J.; Michaelsen, J.; Funk, C. Use of the Gamma Distribution to Represent Monthly Rainfall in Africa for Drought Monitoring Applications. *Int. J. Climatol.* **2007**, *27*, 935–944. [CrossRef]
74. Hosking, J.R.M.; Wallis, J.R. *Regional Frequency Analysis*; Cambridge University Press: Cambridge, UK, 1997.
75. Quesada-Hernández, L.E.; Calvo-Solano, O.D.; Hidalgo, H.G.; Pérez-Briceño, P.M.; Alfaro, E.J. Dynamical Delimitation of the Central American Dry Corridor (CADC) Using Drought Indices and Aridity Values. *Prog. Phys. Geogr.* **2019**, *43*, 627–642. [CrossRef]
76. Gómez Díaz, J.D.; Monterroso Rivas, A.I.; Lechuga Gayosso, L.M. Frecuencia y severidad de la sequía en la Península de Yucatán como instrumento para el ordenamiento del territorio. In *Clima, Sociedad, Riesgos y Ordenación del Territorio*; Asociación Española de Climatología: Sevilla, Spain, 2016; pp. 525–533, ISBN 978-84-16724-19-2.
77. Sheffield, J.; Wood, E.F.; Roderick, M.L. Little Change in Global Drought over the Past 60 Years. *Nature* **2012**, *491*, 435–438. [CrossRef]
78. Van Loon, A.F. Hydrological Drought Explained. *WIREs Water* **2015**, *2*, 359–392. [CrossRef]
79. Svoboda, M.; LeComte, D.; Hayes, M.; Heim, R.; Gleason, K.; Angel, J.; Rippey, B.; Tinker, R.; Palecki, M.; Stooksbury, D.; et al. The Drought Monitor. *Bull. Am. Meteorol. Soc.* **2002**, *83*, 1181–1190. [CrossRef]
80. Stagge, J.H.; Tallaksen, L.M.; Gudmundsson, L.; Van Loon, A.F.; Stahl, K. Candidate Distributions for Climatological Drought Indices (SPI and SPEI). *Int. J. Climatol.* **2015**, *35*, 4027–4040. [CrossRef]
81. Blain, G.C.; De Avila, A.M.H.; Pereira, V.R. Using the Normality Assumption to Calculate Probability-based Standardized Drought Indices: Selection Criteria with Emphases on Typical Events. *Int. J. Climatol.* **2018**, *38*, e418–e436. [CrossRef]
82. Beguería, S.; Vicente-Serrano, S.M.; Reig, F.; Latorre, B. Standardized Precipitation Evapotranspiration Index (SPEI) Revisited: Parameter Fitting, Evapotranspiration Models, Tools, Datasets and Drought Monitoring. *Int. J. Climatol.* **2014**, *34*, 3001–3023. [CrossRef]
83. Livada, I.; Assimakopoulos, V.D. Spatial and Temporal Analysis of Drought in Greece Using the Standardized Precipitation Index (SPI). *Theor. Appl. Climatol.* **2007**, *89*, 143–153. [CrossRef]
84. Le, M.H.; Perez, G.C.; Solomatine, D.; Nguyen, L.B. Meteorological Drought Forecasting Based on Climate Signals Using Artificial Neural Network—A Case Study in Khanhhoa Province Vietnam. *Procedia Eng.* **2016**, *154*, 1169–1175. [CrossRef]
85. Valdés-Rodríguez, O.A.; Salas-Martínez, F.; Palacios-Wassenaar, O.; Marquez, A. Assessment of Corn Grain Production Under Drought Conditions in Eastern Mexico Through the North American Drought Monitor. *Atmosphere* **2025**, *16*, 193. [CrossRef]
86. Hayes, M.; Svoboda, M.; Wall, N.; Widhalm, M. The Lincoln Declaration on Drought Indices: Universal Meteorological Drought Index Recommended. *Bull. Am. Meteorol. Soc.* **2011**, *92*, 485–488. [CrossRef]
87. Wilhite, D.A.; Glantz, M.H. Understanding the Drought Phenomenon: The Role of Definitions. *Plan. Drought Reduct. Soc. Vulnerability* **2019**, *10*, 11–27. [CrossRef]
88. Prasanna, V. Regional Climate Change Scenarios over South Asia in the CMIP5 Coupled Climate Model Simulations. *Meteorol. Atmos. Phys.* **2015**, *127*, 561–578. [CrossRef]
89. Lobell, D.B.; Field, C.B. Global Scale Climate–Crop Yield Relationships and the Impacts of Recent Warming. *Environ. Res. Lett.* **2007**, *2*, 014002. [CrossRef]

90. Sheffield, J.; Wood, E.F. Projected Changes in Drought Occurrence under Future Global Warming from Multi-Model, Multi-Scenario, IPCC AR4 Simulations. *Clim. Dyn.* **2008**, *31*, 79–105. [CrossRef]
91. Lloyd-Hughes, B.; Saunders, M.A. A Drought Climatology for Europe. *Int. J. Climatol.* **2002**, *22*, 1571–1592. [CrossRef]
92. McKee, T.B. Drought Monitoring with Multiple Time Scales. In Proceedings of the 9th Conference on Applied Climatology, Dallas, TX, USA, 15–20 January 1995.
93. Mishra, A.K.; Singh, V.P. A Review of Drought Concepts. *J. Hydrol.* **2010**, *391*, 202–216. [CrossRef]
94. Daly, C.; Halbleib, M.; Smith, J.I.; Gibson, W.P.; Doggett, M.K.; Taylor, G.H.; Curtis, J.; Pasteris, P.P. Physiographically Sensitive Mapping of Climatological Temperature and Precipitation across the Conterminous United States. *Int. J. Climatol.* **2008**, *28*, 2031–2064. [CrossRef]
95. Saxton, K.E.; Rawls, W.J. Soil Water Characteristic Estimates by Texture and Organic Matter for Hydrologic Solutions. *Soil Sci. Soc. Am. J.* **2006**, *70*, 1569–1578. [CrossRef]
96. World Meteorological Organization. *Guidelines on the Definition and Characterization of Extreme Weather and Climate Events*; World Meteorological Organization: Geneva, Switzerland, 2023.
97. Lu, J.; Carbone, G.J.; Gao, P. Detrending Crop Yield Data for Spatial Visualization of Drought Impacts in the United States, 1895–2014. *Agric. For. Meteorol.* **2017**, *237–238*, 196–208. [CrossRef]
98. Zhai, J.; Mondal, S.K.; Fischer, T.; Wang, Y.; Su, B.; Huang, J.; Tao, H.; Wang, G.; Ullah, W.; Uddin, M.J. Future Drought Characteristics through a Multi-Model Ensemble from CMIP6 over South Asia. *Atmos. Res.* **2020**, *246*, 105111. [CrossRef]
99. Tirivarombo, S.; Osupile, D.; Eliasson, P. Drought Monitoring and Analysis: Standardised Precipitation Evapotranspiration Index (SPEI) and Standardised Precipitation Index (SPI). *Phys. Chem. Earth Parts ABC* **2018**, *106*, 1–10. [CrossRef]
100. Cammalleri, C.; Naumann, G.; Mentaschi, L.; Formetta, G.; Forzieri, G.; Gosling, S.; Bisselink, B.; De Roo, A.; Feyen, L. *Global Warming and Drought Impacts in the EU*; Publications Office of the European Union: Luxembourg, 2020.
101. Zhang, R.; Chen, Z.-Y.; Xu, L.-J.; Ou, C.-Q. Meteorological Drought Forecasting Based on a Statistical Model with Machine Learning Techniques in Shaanxi Province, China. *Sci. Total Environ.* **2019**, *665*, 338–346. [CrossRef]